Deciphering myeloid (progenitor) cell function and communication in (tumor) tissues

Lei, X.

Chapter 5

Human progenitor-derived cDC1-like cells as a platform to detect and optimize CTL-based anti-tumor immunity

---

Xin Lei[1], Yizhi Wang[1], Tom de Wit[1], Joanna Grabowska[2], Ellen Schrama[1], Miriam de Boer[1], Jitske van den Bulk[3], Jan Wouter Drijfhout[1], Chong Sun[4], Ton Schumacher[5], Noel F. C. C. de Miranda[3], Jannie Borst[1], Yanling Xiao[1]

[1]Department of Immunology and Oncode Institute, Leiden University Medical Center, Leiden, The Netherlands. [2]Department of Pathology, Leiden University Medical Center, Leiden, The Netherlands. [3]Department of Cell and Chemical Biology, Leiden University Medical Center, Leiden, The Netherlands. [4]Immune Regulation in Cancer, German Cancer Research Center, Heidelberg, Germany. [5]Department of Molecular Oncology and Immunology, The Netherlands Cancer Institute, Amsterdam, The Netherlands.

Manuscript in preparation

Abstract

Classical type 1 dendritic cells (cDC1) play a pivotal role in anti-tumor immunity by regulating $CD8^+$ T-cell activation in both tumor-draining lymph nodes and the tumor microenvironment. Efficacy of cancer therapy with adoptively transferred T-cells can be optimized by engaging cDC1. *In vivo*, the cDC1 activates tumor-specific $CD8^+$ T-cells *de novo* and induces adequate effector differentiation of tumor-specific $CD8^+$ T-cells. Presently, scarcity of primary cDC1 hinders their application in *in vitro* strategies. We present here a method to generate cDC1-like cells resembling *ex vivo* cDC1 in high yield from $CD34^+$c-Kit^+ hematopoietic progenitor cells, as isolated from non-mobilized adult blood. We demonstrate that the *in vitro* generated cDC1-like cells resemble *ex vivo* cDC1 in their response to $CD4^+$ T-cell help signals, which optimize their antigen cross-presentation and cytotoxic T lymphocyte (CTL) priming capacity. We show that *in vitro* generated and helped cDC1-like cells can be used for two therapeutically relevant goals: 1) to enhance the cytotoxic potency of tumor-specific CTL and 2) to enable the detection of scarce tumor antigen-specific $CD8^+$ T-cells in human blood. For these reasons, our *in vitro* cDC1 culture platform that incorporates $CD4^+$ T-cell help presents a strategy to optimize adoptive T-cell therapies of cancer.

Key words:

progenitor, *in vitro* cDC1-like cell generation, tumor antigen-specific $CD8^+$ T-cells, immunotherapy

Introduction

Classical dendritic cells (DC) are antigen presenting cells that function as sentinels of the immune system[1]. They patrol peripheral tissues, where they phagocytose cell debris and sense signals of infection or danger through pattern recognition receptors (PRR)[2]. They travel to lymph nodes, where they can induce T-cell tolerance or immunity, depending on their activation state. The DC lineage encompasses plasmacytoid (p)DC and classical (c) DC[3,4] subsets, of which the latter is subdivided into cDC1 and cDC2[5]. DC develop under homeostatic conditions in the bone marrow (BM) from hematopoietic progenitor cells (HPC), wherein fms-related receptor tyrosine kinase 3 (FLT3) is a key driver cytokine[6]. These DC lineages are distinct from monocyte-derived DC (moDC), which are generated under inflammatory conditions[3,7,8]. The development of DC subsets is linked to distinct transcription factor (TF) networks, such as *ZEB2* for pDC, *IRF8* and *BATF3* for cDC1, and *IRF4* for cDC2 and moDC[4,9,10]. Additionally, these DC lineages can be distinguished by their key surface markers, including CD123 and CD303 for pDC, CD141, XCR1 and CLEC9A for cDC1, CD1c and SIRPRα for cDC2, and CD14 and CD1a for moDC[4,11].

Among the DC lineages, cDC have the unique ability to transport antigens from peripheral tissues to draining lymph nodes (dLN) to initiate T-cell activation[12,13]. Specifically, cDC1 excel in cross-presentation of phagocytosed cell-associated antigens in MHC class I to activate $CD8^+$ T-cells[14]. Recent data indicate that in tumor settings, cDC1 can also maintain a reservoir of primed, stem-like $CD8^+$ T-cells in the tumor (t) dLN[15] and shape T-cell states in the tumor microenvironment (TME)[16–19]. The cDC1 subset is also unique in its ability to respond to antigen-specific $CD4^+$ T-cell help, a process known as DC licensing, that augments survival, maturation, migration and antigen presentation abilities of the cDC1[19,20]. In mouse and human tumor settings, it has been shown that helped/licensed cDC1 in turn promote clonal expansion, effector- and memory differentiation of $CD8^+$ T-cells both in tdLN[21–24] and the TME[19]. By these mechanisms, cDC1 play a pivotal role in cytotoxic T-lymphocyte (CTL) mediated anti-tumor immunity[22,25–27] and are highly attractive targets or tools in cancer immunotherapy.

Immune checkpoint blockade (ICB), primarily PD-(L)1 blockade, has shown clinical benefit, but only in cancer types that spontaneously become infiltrated with tumor-specific CTL[28–31]. Particularly for cancer types that are immunosuppressive or not immunogenic, adoptive T-cell transfer therapy (ACT) is a promising avenue, for which tumor-infiltrating lymphocytes (TIL)[32] can be used, or T cells genetically endowed with tumor-specific antigen receptors[33]. Identification of tumor-reactive T-cells, their

antigenic specificities and cognate T cell antigen receptor (TCR) have led to next-generation therapeutic T-cell engineering. Fluorescent[34] or metal-labeled[35] multimers of Major Histocompatibility Complex (MHC) class I molecules, loaded with tumor antigen-derived peptides are used to identify tumor-specific $CD8^+$ T-cells among TIL. Additionally, tumor-specific CTL are identified based on phenotypic markers, such as PD-1[36] or CD39[35], or production of effector cytokines such as IFNγ[37]. TILs represent an enriched source of tumor-reactive T-cells, but this material is not readily available for all patients. Alternatively, circulating T-cells represent another source for tumor-reactive T-cell identification, but their low frequency is an obstacle[38–40]. Therefore, there is a need for more sensitive methods to identify tumor-specific T-cells in peripheral blood. Moreover, patients may develop resistance to ACT, due to limitations in antigen recognition or functional activity[41–43]. Therefore, it is important to develop strategies to enhance the anti-tumor effector function of engineered T-cells. In both identification of tumor-specific $CD8^+$ T cells and the optimization of their function, cDC1 can play an important role.

The frequency of cDC1 in human blood is only 0.02%[19], with significant interindividual variations, which makes it difficult to harvest them for clinical use. This problem can potentially be solved by generating cDC1-like cells from HPC *in vitro*, provided that the key drivers of their differentiation trajectory are known. Apart from Flt3 signaling, delta-like ligand 1 (DLL1)-mediated Notch signaling was recently discovered as driver of murine[44] and human[45] cDC1 development from progenitor cells. This finding has created a new opportunity to make cDC1-like cells *in vitro*, but the cell yields were still suboptimal. Although *in vitro*-generated cDC1-like cells do express key cell surface markers of *ex vivo* cDC1, such as XCR1 and CLEC9A, they are also reported to express other markers, such as CD1c, which contrasts with their blood counterparts[45]. In these novel protocols[44,45], the hematopoietic progenitors were isolated from either BM, cord blood or mobilized adult blood, which are challenging sources in case of cancer patients. We here report a modified method to generate cDC1-like cells in high-yield from $CD34^+$c-Kit^+ HPC derived from non-mobilized adult blood. These cells share key phenotypic and functional traits with primary, *ex vivo* cDC1. Most importantly, we demonstrate their ability to relay help that optimizes tumor-specific CTL priming and enables the sensitive detection of very low frequency tumor antigen-specific $CD8^+$ T cells in healthy human blood.

Results

In vitro generation of human cDC1-like cells from adult blood-derived progenitors

The currently most effective protocol to generate human cDC1-like cells uses as cell of origin HPC from BM or cord blood[45]. We explored the use of HPC from non-mobilized adult blood, as this would be applicable to cancer patients. To establish the protocol, $CD34^+$c-Kit^+ progenitor cells were isolated from peripheral blood mononuclear cells (PBMC) of healthy donors (**Fig. S1A, Fig. 1A**). From 100 million PBMC, on average about 15000 progenitors could be isolated (**Fig. 1B**). The sorted progenitors were cultured on mesenchymal stem cells (MSC)[46,47] in the presence of FLT3L, stem cell factor (SCF), thrombopoietin (TPO), macrophage colony-stimulating factor (M-CSF), granulocyte-macrophage colony-stimulating factor (GM-CSF) and interleukin-7 (IL-7). The cytokine cocktail for DC expansion and differentiation was based on published work[46] and our own previous work[48]. We cultured the progenitor cells on a layer of OP9 cells expressing human (h)DLL1 to engage Notch signaling as described[45,46]. In our modified protocol, we also used MSC in the feeder layer in a 1:1 ratio (**Fig. S1B, Fig. 1C**). MSC are stromal cells that are a key part of the BM microenvironment[46]. They provide growth factors that support HPC expansion and differentiation, including SCF, Flt3L and GM-CSF[47] and we found earlier a beneficial role of MSC in generating DC from HPC[48]. At the end of the 14-day culture, cDC1 were phenotypically identified by flow cytometry (**Fig. S1C**). Cells expanded about 100-fold during the culture process (**Fig. 1D** and **E**). About 60% of the live cell yield consisted of $CD3^-CD19^-$HLA-DR^+CD88^- DC (**Fig. S1C** and **D**)**.** CD88 was used for gating out moDC. CLEC9A, IRF8, XCR1, CD141, and CD226 were used to identify cDC1-like cells, while CD14 and SIRPα were used for cDC2-like cell identification. Within the DC progeny, we defined cDC1-like cells as a HLA-DR^+ $CD11c^+CLEC9A^+IRF8^+$ population with variable expression of XCR1, CD141 and CD226 and low or no expression of surface markers defining cDC2, pDC and moDC, including CD14 and SIRPα (**Fig. 1F** and **G; Fig. S1E**). Overall, DC progeny comprised approximately 60~70% cDC1-like cells, and one progenitor could generate ~45 cDC1-like cells (**Fig. 1H**). This was ~5 to 7 times higher than previously published protocols[45,49].

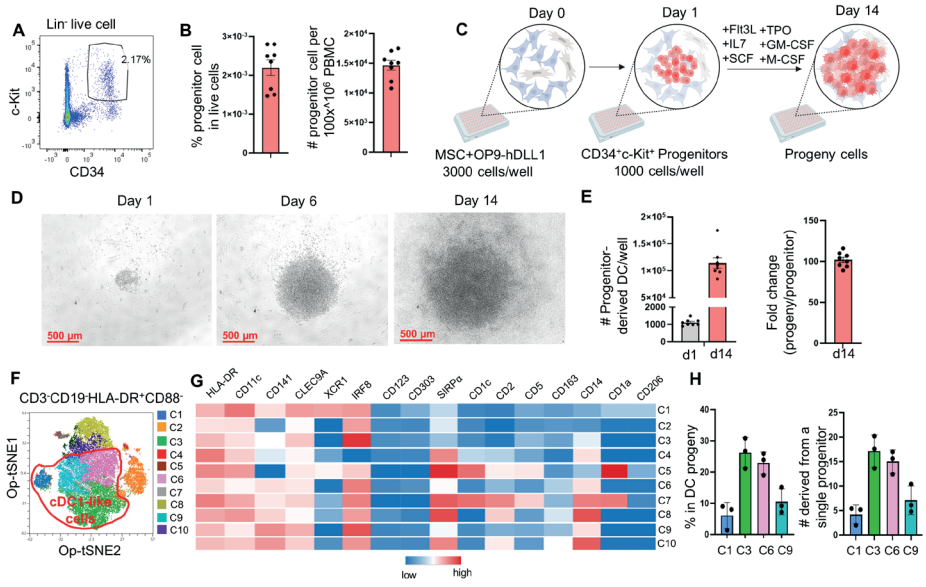

Fig. 1 Generating human cDC1-like cells from non-mobilized blood-derived progenitors in vitro. CD34^{+}c-Kit^{+} progenitor cells were isolated from PBMC by flow cytometric sorting, then cultured with a cytokine cocktail for 14-21 days. Mesenchymal stromal cells (MSC) and OP9 expressing human delta-like ligand 1 (hDLL1) were used as feeder cells. (**A**) Gating strategy for progenitor cell isolation from PBMC. (**B**) Frequencies (%) of progenitor cells in live cells and absolute numbers (#) of progenitor cells isolated per 100x10^{6} PBMC. (**C**) Schematic illustration of in vitro progenitor-derived DC differentiation. (**D**) Microscopic pictures depicting the growth of progenitor-derived DC. (**E**) # of progenitor cells on day 1 and progeny cells on day 14, and the fold change of progeny versus progenitor cells. (**F**) Op-tSNE plot of 10 clusters identified within HLA-DR^{+}CD88^{-} population. Red line indicates clusters (C1, 3, 6, 9) of cDC1-like cells. (**G**) Heatmap of median expression values of key phenotypic markers identifying cDC1. (**H**) % of cDC1-like cells in HLA-DR^{+}CD88^{-} DC progeny and # of cDC1-like cells derived from a single progenitor cell. Data are pooled from eight (n=8) independent donors in **B** and **E;** data are pooled from three independent donors (n=3) in **H**. Data are shown as means ± standard error of mean (SEM).

Progenitor-derived DC respond to activated CD4$^+$ T-cells

We have previously demonstrated that *ex vivo* human cDC1 exhibit a unique response to activated CD4$^+$ T-cells, upregulating multiple pathways that are important for antigen cross-presentation and T-cell priming[19]. This setting mimics CD4$^+$ T-cell help as it occurs *in vivo*, where the CD4$^+$ T-cell recognizes antigen on the cDC1. In our system, we mimic this event by activating the CD4$^+$ T-cell with agonistic monoclonal antibody to CD3. To test whether our progenitor-derived DC resembled *ex vivo* cDC1 in this aspect, we assessed the response of progenitor-derived DC to activated versus naïve CD4$^+$ T-cells (**Fig. 2A**). Upon stimulation with activated CD4$^+$ T-cells, progenitor-derived DC, identified as a CD3$^-$HLA-DR$^+$ population, significantly increased the expression of costimulatory/coinhibitory molecules CD40, CD70, CD80, CD83, CD86 and PD-L1 (**Fig. 2C** and **D**), chemokine receptor CCR7 and chemokines CXCL9/10, antigen presentation pathway components including the transporter associated with antigen presentation (TAP1/2), β2-microglobulin(M), HLA-A/B/C and MHC class II molecules HLA-DR (**Fig. 2E** and **F**). These are the molecules that we previously found to be upregulated on primary *ex vivo* cDC1 from human blood after co-culture with activated CD4$^+$ T cells[19] and that are part of the *in vivo* cDC1 licensing program in human and mouse[19,50]. Additionally, progenitor-derived DC also responded to pattern recognition receptor (PRR) stimuli. Activated CD4$^+$ T-cells and PRR stimuli partially induced similar changes in expression of abovementioned molecules in progenitor-derived DC (**Fig. S2**). However, "helped" DC had higher expression of chemokines CXCL9/10 and components of the MHC class I antigen presentation pathway (**Fig. S2**). Hence, progenitor-derived DC similarly responded to activated CD4$^+$ T-cells and PRR stimuli as their *ex vivo* cDC1 counterpart[19].

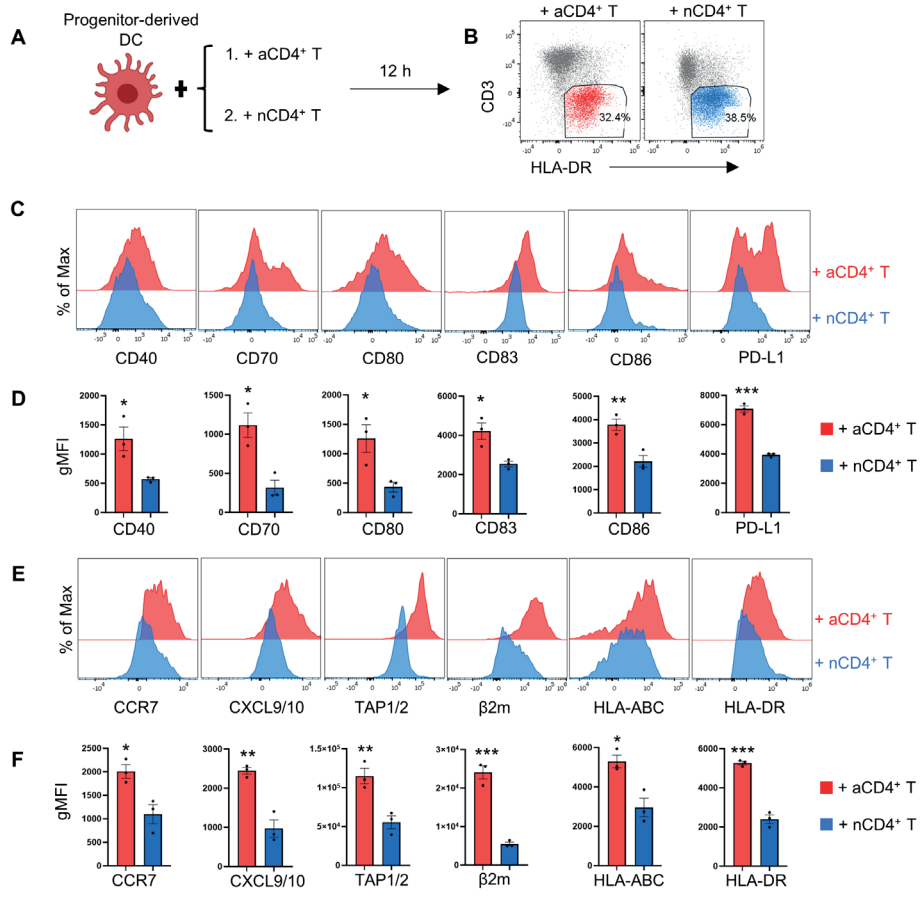

Fig. 2. Response of in vitro progenitor-derived DC to activated CD4⁺ T-cells. Total progenitor-derived DC were co-cultured with activated (a)- or naïve (n)CD4⁺ T-cells overnight. Next, key molecules of the cDC1 "help" signature were analyzed by flow cytometry[19]. (**A**) Illustration of the experimental design. (**B**) Gating strategy for flow cytometric analysis of progenitor-derived DC after co-culture. (**C-F**) Histograms (**C** and **E**) and geometric mean fluorescence index (gMFI) quantifications (**D** and **F**) for indicated markers expressed by progenitor-derived DC under indicated conditions. Data are pooled from three (n=3) independent donors in **D** and **F**, and are shown as means ± SEM. p<0.05*, p<0.01**, p<0.001*** (two-sided unpaired Student's t-test).

Progenitor-derived DC can relay CD4⁺ T-cell help for priming of tumor-specific CTL

CD4⁺ T-cell help endows the cDC1 with the optimal abilities to prime tumor-specific CTLs[19,22]. Therefore, we investigated the capability of progenitor-derived DC to relay CD4⁺ T-cell help for CD8⁺ T-cell (cross)priming in our *in vitro* CTL priming platform[19]. For this purpose, CD8⁺ T-cells from peripheral blood are transduced to express a T-cell receptor

(TCR) specific for MART-1_{26-35} peptide in the context of HLA-A2. This allows them to act as responder cells in the assay. HPC are isolated from HLA-$A2^+$ donors and progenitor-derived DC are generated from them. These DC are first cultured with either naïve or activated $CD4^+$ T-cells before antigen loading. Next, the DC are loaded with either MART-1_{26-35} short peptide (SP), or MART-1_{15-40} long peptide (LP), or MART-1 expressing dead melanoma 526[19] (Mel526) cell debris were used as antigen source. These antigen sources require no processing and direct presentation in the case of short peptide and limited or extensive processing and cross-presentation in the other two cases. During antigen loading, DC are additionally activated with a mixture of PRR stimuli (poly I:C, LPS and R848). Cell Trace Violet (CTV) labeled $CD8^+$ T-cells are added into the co-culture 12 h after antigen loading (**Fig. 3A**). This platform can reliably report the ability of DC to prime T-cells, based on CTV dilution and Granzyme B production in TCR-transduced $CD8^+$ T-cells (**Fig. S3A**). In the SP setting, progenitor-derived DC induced robust MART-1_{26-35} -specific $CD8^+$ T-cell responses both in terms of proliferation (**Fig. 3B**) and Granzyme B induction (**Fig. 3C**), irrespective of the presence of $CD4^+$ T-cell help. Nonetheless, a slight but significant enhancement in CTL priming was observed when activated $CD4^+$ T-cells were present (**Fig. 3B** and **C**). In the cross-presentation setting with MART-1_{15-40} long peptide, CTL responses were much more significantly increased when DC were "helped" by activated $CD4^+$ T-cells (**Fig. 3D** and **E**). In the cross-presentation setting with Mel526 cell debris, progenitor-derived DC were able to phagocytose GFP^+ melanoma cell debris, as indicated by co-expression of GFP, CD45 and CD11c assessed by imaging flow cytometry (**Fig. S3B-D**). Only DC co-cultured with activated $CD4^+$ T-cells ("helped" DC) induced MART-1_{26-35} -specific $CD8^+$ T-cell proliferation (**Fig. 3F**) and Granzyme B production (**Fig. 3G**), whereas DC co-cultured with naïve $CD4^+$ T-cells ("non-helped" DC) failed to do so (**Fig. 3F** and **G**). Interestingly, proliferation was also observed in HLA-A2/MART-1_{26-35} tetramer-negative $CD8^+$ T-cells, indicating progenitor-derived DC are capable to prime $CD8^+$ T-cells specific for tumor antigens, other than MART-1_{26-35} antigen (**Fig. 3F**). In addition, phagocytosis of GFP^+ melanoma cell debris was observed by co-expression of GFP, CD45 and CD11c using imaging flow cytometry (**Fig. S3B-D**). Hence, similar to *ex vivo* cDC1[19], progenitor-derived DC responded to $CD4^+$ T-cell help by optimizing their CTL (cross)priming ability.

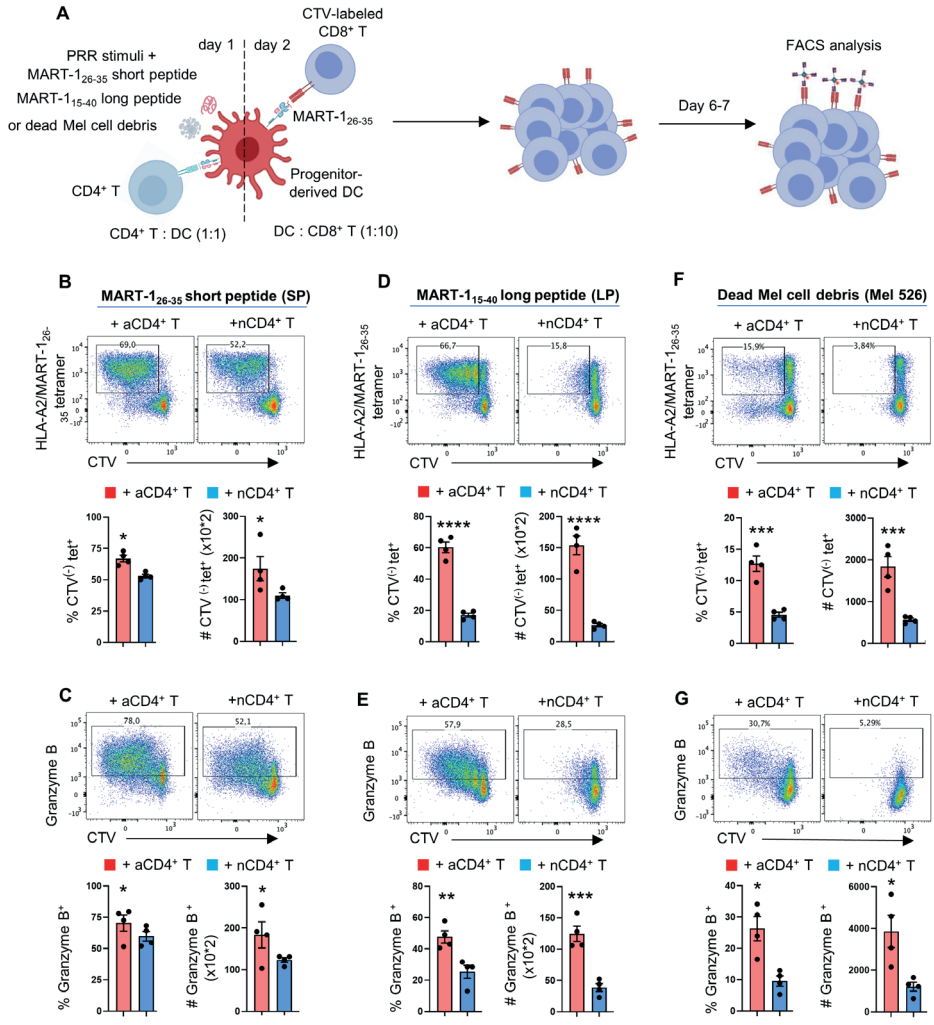

Fig. 3 Progenitor-derived DC has the ability to relay CD4⁺ T-cell help for CTL responses. (**A**) Scheme of the tumor antigen-specific CTL priming system. On day 1, ~5,000 total progenitor-derived DC from HLA-A2⁺ healthy donors were incubated with equal numbers of activated (a)- or naïve (n)CD4⁺ T-cells, loaded with MART-1 peptide antigens or dead MART-1⁺ melanoma cell debris and a mixture of PRR stimuli. On day 2, ~50,000 CD8⁺ T-cells that had been transduced to express the MART-1_{26-35}/HLA-A2-specific TCR with T_{SCM} phenotype[19] were added. The T-cell response was read out at day 6 or 7 after co-culture. (**B, D, F**) CD8⁺ T-cell proliferation to (**B**) MART-1_{26-35} short peptide (SP), (**D**) MART-1_{15-40} long peptide (LP) or (**F**) dead Mel526 cell debris based on CTV dilution. Upper panel, primary flow cytometric data. Lower panel, frequency (%) of MART-1_{26-35}/HLA-A2-specific (tet⁺) cells within CTV(-) CD8⁺ T-cells, and their absolute, live cell number (#). (**C, E, G**) CTL response to (**C**) MART-1_{26-35} SP, (**E**) MART-1_{15-40} LP or (**G**) dead Mel526 cell debris based on intracellular Granzyme B staining. Upper panel, primary flow cytometric data. Lower panel, frequency of Granzyme B⁺ cells among CD8⁺ T-cells, and their absolute, live cell number. Data are pooled from four (n=4) independent experiments, are shown as means ± SEM. p<0.05*, p<0.01**, p<0.001*** (two-sided unpaired Student's t-test).

Improved detection of tumor antigen-specific CD8$^+$ T-cells in healthy donor blood with "helped" progenitor-derived DC

We next investigated whether we could use the CTL priming platform with progenitor-derived DC to detect CD8$^+$ T-cells specific for tumor antigens in peripheral blood of healthy donors. We explored T-cell specificity for four HLA-A2-restricted melanoma-derived antigens, including tumor-associated antigens (TAA) and mutation-derived neoantigens (**Fig. 4SA**), as proof of principle. DC and T-cells from the same HLA-A2$^+$ healthy donors were used in the CTL priming platform, debris of dead Mel526 cells expressing both MART-1$_{26\text{-}35}$ and CDK4$_{23\text{-}32}$ was used as antigen source (**Fig. 4A**). After 6 days of co-culture, CD8$^+$ T-cells against specific epitopes were detected using peptide/MHC-I tetramers in combination with T-cell activation markers (**Fig. S4A** and **B**). HLA-A2/MART-1$_{26\text{-}35}$ and HLA-A2/CDK4$_{23\text{-}32}$ tetramers conjugated with two different fluorochromes were used to increase the specificity. In the "no help" setting with naïve CD4$^+$ T-cells, we detected CD8$^+$ T-cells specific for HLA-A2/MART-1$_{26\text{-}35}$ in our assay with progenitor-derived DC, in a frequency of 0.14%±0.03% (**Fig. 4B** and **C**). In the "help" setting with activated CD4$^+$ T-cells, significantly more HLA-A2/MART-1$_{26\text{-}35}$ tet$^+$CD8$^+$ T-cells were detected, in a frequency of 0.42%±0.04% (**Fig. 4B** and **C**). Similar results were obtained for CD8$^+$ T-cells specific for HLA-A2/CDK4$_{23\text{-}32}$. Detection of HLA-A2/CDK4$_{23\text{-}32}$ tet$^+$CD8$^+$ T-cells had a five-fold increase in the "help" setting (0.25%±0.03%) compared to the "no help" setting (0.05%±0.01%) (**Fig. 4H** and **I**). Correspondingly, the absolute cell numbers of HLA-A2/MART-1$_{26\text{-}35}$- or HLA-A2/CDK4$_{23\text{-}32}$ tet$^+$CD8$^+$ T-cells was significantly higher in the "help" setting (**Fig. 4C** and **I**). Importantly, CTL effector differentiation of tumor antigen-specific CD8$^+$ T-cells was increased in the "help" setting, according to increased CD45RO and Granzyme B expression (**Fig. 4D, E, J** and **K**). These results were further validated by the quantifications of both frequencies and cell numbers of CD45RO$^+$CTV$^{(-)}$tet$^+$ T-cells (**Fig. 4F, G, L** and **M**). We also detected more total and proliferative CD8$^+$ T-cells specific for HLA-A2/gp100$_{280\text{-}288}$ and HLA-A2/MAGE3$_{271\text{-}279}$ in the "help" setting (**Fig. S4C-F**). Overall, these results indicate that the *in vitro* platform using CD4$^+$ T-cell "help" relayed via progenitor-derived DC can be used to increase detection of primary tumor-specific CD8$^+$ T-cells in peripheral blood. This platform can be created using autologous HPC, CD4$^+$ T-cell and CD8$^+$ T-cells from blood of adult healthy donors or cancer patients.

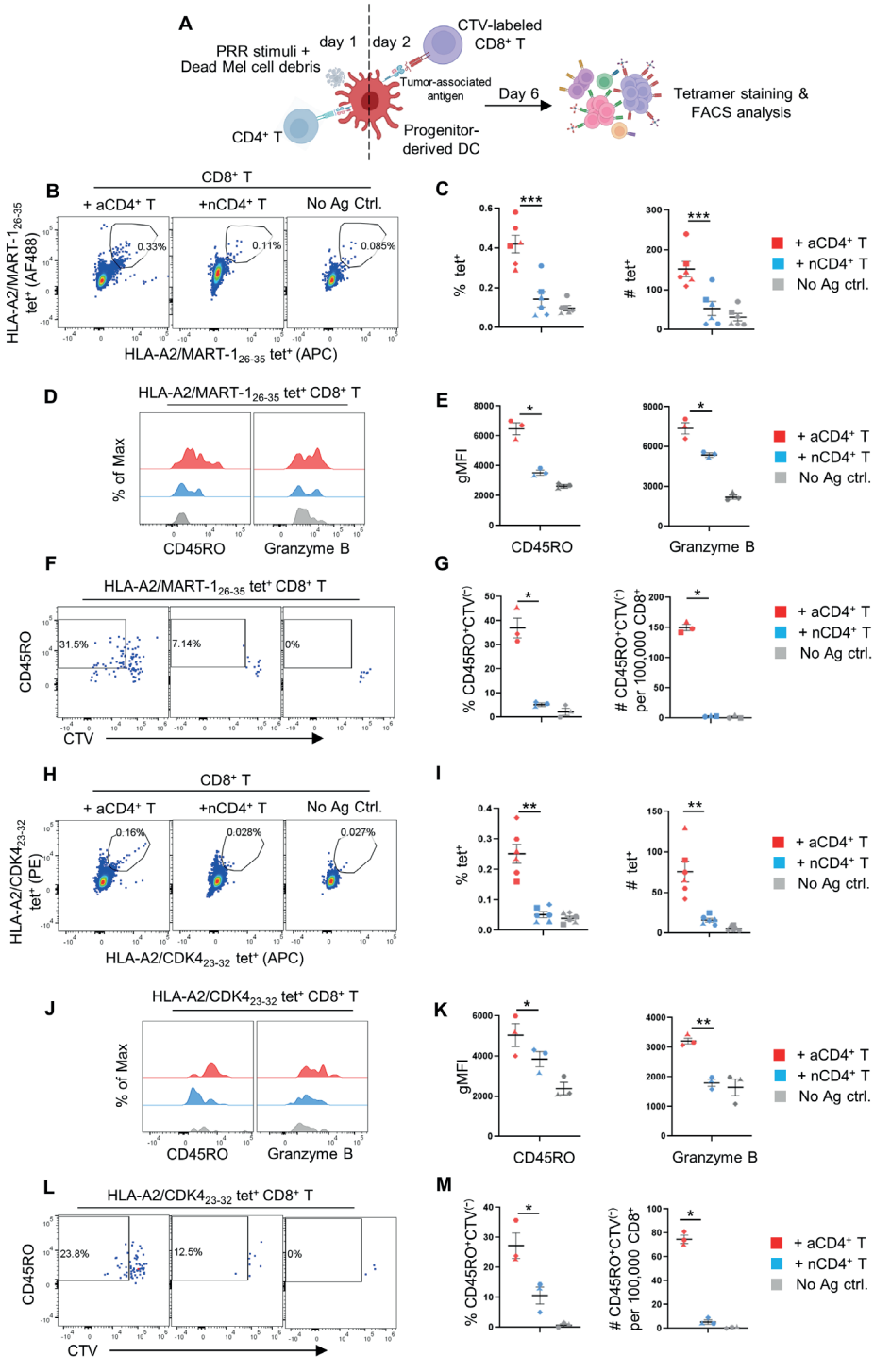
A
PRR stimuli +
Dead Mel cell debris
day 1
day 2
CTV-labeled
CD8+ T
Tumor-associated
antigen
Day 6
Tetramer staining &
FACS analysis
CD4+ T
Progenitor-
derived DC
B
CD8+ T
+ aCD4+ T
+nCD4+ T
No Ag Ctrl.
0.33%
0.11%
0.085%
HLA-A2/MART-126-35
tet+ (AF488)
HLA-A2/MART-126-35 tet+ (APC)
C
% tet+
# tet+
+ aCD4+ T
+ nCD4+ T
No Ag ctrl.
D
HLA-A2/MART-126-35 tet+ CD8+ T
% of Max
CD45RO
Granzyme B
E
gMFI
CD45RO
Granzyme B
F
HLA-A2/MART-126-35 tet+ CD8+ T
CD45RO
31.5%
7.14%
0%
CTV
G
% CD45RO+CTV(-)
# CD45RO+CTV(-)
per 100,000 CD8+
H
CD8+ T
+ aCD4+ T
+nCD4+ T
No Ag Ctrl.
0.16%
0.028%
0.027%
HLA-A2/CDK423-32
tet+ (PE)
HLA-A2/CDK423-32 tet+ (APC)
I
% tet+
# tet+
J
HLA-A2/CDK423-32 tet+ CD8+ T
% of Max
CD45RO
Granzyme B
K
gMFI
CD45RO
Granzyme B
L
HLA-A2/CDK423-32 tet+ CD8+ T
CD45RO
23.8%
12.5%
0%
CTV
M
% CD45RO+CTV(-)
# CD45RO+CTV(-)
per 100,000 CD8+

Fig. 4 Detection of tumor antigen-specific CD8$^+$ T-cells in healthy donor blood with "helped" progenitor-derived DC. Per assay, ~50,000 CD8$^+$ T-cells sorted from PBMC were co-cultured with ~5,000 progenitor-derived DC loaded with dead Mel526 cell debris in presence of ~5,000 activated (a)- or naïve (n)CD4$^+$ T-cells. Tumor antigen-reactive CD8$^+$ T-cells were detected using peptide/MHC-I tetramers and T-cell activation markers. (**A**) Experimental design. (**B**) Flow cytometric plots depict CD8$^+$ T-cells specific for HLA-A2/MART-1$_{26-35}$. (**C**) Frequency (%) of MART-1$_{26-35}$-specific cells within total CD8$^+$ T-cells, and total number (#) of MART-1$_{26-35}$-specific CD8$^+$ T-cells. (**D** and **E**) Histogram (**D**) and gMFI quantifications (**E**) for CD45RO and Granzyme B expressed by MART-1$_{26-35}$-specific CD8$^+$ T-cells under indicated conditions. (**F**) Flow cytometric plots depict the MART-1$_{26-35}$-specific CD45RO$^+$CTV$^{(-)}$CD8$^+$ T-cells. (**G**) Frequency of CD45RO$^+$CTV$^{(-)}$ cells within MART-1$_{26-35}$-specific CD8$^+$ T-cells and their absolute number (#). (**H**) Flow cytometric plots depict CD8$^+$ T-cells specific for HLA-A2/CDK4$_{23-32}$. (**I**) Frequency of CDK4$_{23-32}$-specific cells within CD8$^+$ T-cells, and their absolute number (#). (**J** and **K**) Histogram (**J**) and gMFI quantifications (**K**) for CD45RO and Granzyme B expressed by CDK4$_{23-32}$-specific CD8$^+$ T-cells under indicated conditions. (**L**) Flow cytometric plots depict the CDK4$_{23-32}$-specific CD45RO$^+$CTV$^{(-)}$CD8$^+$ T-cells. (**M**) Frequency of CD45RO$^+$CTV$^{(-)}$ cells within CDK4$_{23-32}$-specific CD8$^+$ T-cells, and their absolute, live cell number (#) per 100,000 total CD8$^+$ T-cells. Data are pooled from six (n=6 in **C, I**), and three (n=3 in **E, G, K, M**) independent donors, and are shown as means ± SEM. P<0.05*, p<0.01**, p<0.001*** (two-sided paired student t test).

Improved generation of tumor-specific CTL from blood-derived CD8$^+$ T-cells with "helped" progenitor-derived DC

We next tested whether the CD4$^+$ T-cell help platform with progenitor-derived DC could be used to expand and differentiate autologous tumor-reactive CTL from CD8$^+$ T-cells in peripheral blood, without knowing their antigen-specificity. We used, as before, dead Mel562 cell debris as tumor antigen source and total polyclonal CD8$^+$ T-cells from healthy adult donor blood as responder cells (**Fig. 5A**). Similar to what we observed using MART-1-specific CD8$^+$ T-cells, DC that had been co-cultured with activated CD4$^+$ T-cells ("helped") were more effective than DC co-cultured with naïve CD4$^+$ T-cells ("non-helped") in inducing CD8$^+$ T-cell priming, both in terms of proliferation (**Fig. 5B** and **C, Fig. S5A** and **B**) and CTL effector differentiation, as indicated by Granzyme B and IFNγ production (**Fig. 5D-G, Figure S5B**). We tested the killing capacity of the CD8$^+$ T-cells that had been primed by DC for 6 days with the IncuCyte platform, which monitors in real-time live/dead cells in captured images and measures target cell killing based on Caspase-3/7 activity. After 24 h of imaging, cells in suspension were analyzed by flow cytometry and Mel526 cells adhering to the culture dish were fixed and stained (**Fig. 5H, Fig. S5C**). Proliferating CTV$^{(-)}$ CD8$^+$ T-cells were considered as tumor-reactive in comparison to CTV$^+$CD8$^+$ T-cells. Total CD8$^+$ T-cells from the no antigen control condition were used as a reference for responders (**Fig. 5I**). Granzyme B production and cell surface expression of granule exocytosis marker CD107α were increased in CTV$^{(-)}$CD8$^+$ T-cells that had been primed by "helped" DC as compared to "non-helped" DC (**Fig. 5J**). Correspondingly, CTV$^{(-)}$CD8$^+$ T-cells derived from the "helped" condition were more capable of killing Mel526 cells, indicated by numbers of total and dead Mel526 cells in the cell suspension (**Fig. 5K** and **I**), quantification of Caspase

3/7 activity (**Fig. 5M**), and confluence of the remaining Mel526 cells (**Fig. 5N**). In contrast, there was limited killing capacity in non-proliferative CTV^{+}CD8^{+} T-cells irrespective of the presence or absence of "help" (**Fig. S6**). Overall, these results indicate that "helped" progenitor-derived DC can efficiently cross-prime tumor-specific and active CTL from a polyclonal repertoire of CD8^{+} T-cells in adult human blood.

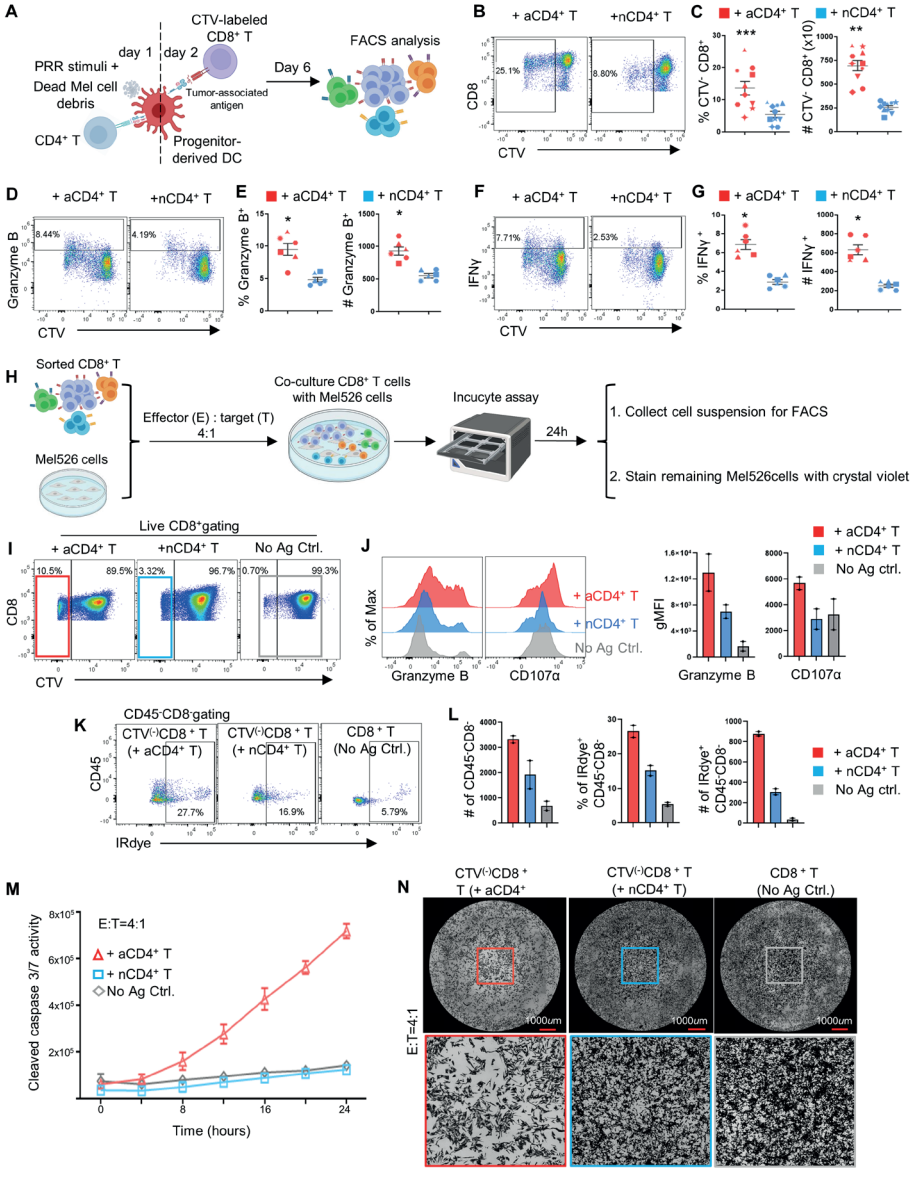

Fig. 5 Improved generation of tumor-specific CTL from blood-derived CD8$^+$ T-cells with "helped" progenitor-derived DC. (A-G) ~50,000 CD8$^+$ T-cells were sorted from PBMC and co-cultured with ~5,000 progenitor-derived DC loaded with dead Mel526 cell debris in presence of ~5,000 activated (a)- or naïve (n)CD4$^+$ T-cells for 6 days, after which the CD8$^+$ T-cell response was measured by flow cytometry. (A) Experimental design. (B) Flow cytometric plots depicting CD8$^+$ T-cell proliferation based on CTV dilution. (C) Frequency of CTV$^{(-)}$ cells within total CD8$^+$ T-cells, and absolute number (#) of live CTV$^{(-)}$CD8$^+$ T-cells. (D and F) Flow cytometric plots depicting the CTL response based on intracellular Granzyme B (D) and IFNγ (F) staining. (E) Frequency of Granzyme B$^+$ cells within total CD8$^+$ T-cells and their absolute, live cell numbers (#). (G) Frequency of IFNγ$^+$ cells within total CD8$^+$ T-cells and their absolute, live cell numbers (#). (H-N) Killing assay was performed using live proliferative (CTV negative) CD8$^+$ T-cells purified from the CTL priming system and Mel526 tumor cells at effector/target (E/T) ratio of 4/1, and analyzed by IncuCyte during 24h. At the end of the assay, the cell suspension was pooled and analyzed by flow cytometry. Remaining Mel526 cells in each well were fixed and stained with crystal violet. (H) Experimental design. (I) Gating strategy for isolating CTV$^{(-)}$CD8$^+$ T-cells from the CTL priming system. Total live CD8$^+$ T-cells from no antigen setting were used as reference. (J) Histograms and gMFI quantifications for Granzyme B and cell surface CD107α expressed by CD8$^+$ T-cells after the killing assay. (K) Flow cytometric plots depicting total and dead Mel526 cells in the cell suspension after the killing assay, as indicated by CD45$^{(-)}$CD8$^{(-)}$ and IRdye$^+$CD45$^{(-)}$ CD8$^{(-)}$ populations under indicated conditions. (L) Total number (#) of tumor cells, frequency and number (#) of dead tumor cells in the cell suspension. (M) Caspase 3/7 activity in tumor cells during the killing assay under the indicated conditions. (N) Representative CCD microscopic images depicting remaining Mel526 cells in the plate at 24h post co-culture under indicated conditions. Data are pooled from eight (n=10 in C) and three (n=6 in E and G) independent donors, and are shown as means ± SEM. P<0.05*, p<0.01**, p<0.001*** (two-sided paired Student's t test in C, E, G). Data are pooled from two (n=2 in J, L and N) independent donors, and are shown as means ± standard deviation (SD).

Discussion

We have established an *in vitro* culture protocol for the efficient generation of cDC1-like cells from HPC derived from adult, non-mobilized blood. The cDC1-like cells produced *in vitro* closely mimic their *ex vivo* cDC1 counterpart in terms of functionality. They exhibit the capacity to relay CD4$^+$ T-cell "help", leading to the effective induction of antigen-specific CTL responses from a polyclonal CD8$^+$ T cell repertoire in peripheral blood of healthy donors. This protocol provides a robust tool for detecting antigen-specific CD8$^+$ T-cells and qualitative improvement of CD8$^+$ T-cell products for immunotherapy.

The key function of DC is to regulate antigen-specific T-cell responses, holding great promise as cellular vaccines for eliciting antigen-specific anti-tumor immune responses. Previous clinical trials have primarily using human moDC for this purpose and had unsatisfactory outcomes, which are attributed to poor homing capacity to LN[51,52] and limited ability to (cross)prime CD8$^+$ T-cells[19]. In contrast, cDC1 migrate effectively from tissues to LN by upregulating chemokine receptor CCR7 upon antigen capture, and are specialized in (cross)presenting cell-associated antigens to CD8$^+$ T-cells[12,13]. Therefore, cDC1 vaccination is highly attractive for immunotherapies. Our robust *in*

vitro DC culture protocol facilitates efficient generation of cDC1-like cells from blood-derived non-mobilized $CD34^+c\text{-}Kit^+$ HPC. Blood is a more accessible source of HPC compared to BM or G-CSF-moblied blood, rendering our protocol more clinically available, particularly for cancer treatments.

Our culture method to make cDC1-like cells from HPC differs from the method of Balan *et al*.[45] primarily by presence of MSC in the feeder layer[48], which provide growth factors for HPC expansion and differentiation[47]. The yield of cDC-like cells per HPC is 5 times higher in our culture system. Since cDC1 frequency in blood is about 0.02%[19], maximally 20,000 primary cDC1 can be isolated from $100x10^6$ PBMC. This underscores the advantage of *in vitro* generation of cDC1-like cells from progenitors over using *ex vivo* cDC1. Further optimization of the culture method can likely be done by using MSC transduced with DLL1 and elimination of OP9 cells. For complete elimination of the feeder cells, we need to know the critical factors provided by MSC.

cDC1 play a critical role in priming anti-tumor CTL responses, but mouse tumor models have indicated an additional role for cDC2, likely for initial activation of $CD4^+$ T helper cells[21]. Recent literature on viral infection suggests that crosstalk between DC subsets can significantly alter biological outcomes[53]. [21]Thus, combined administration of cDC1 and cDC2 as cancer immunotherapy may be appealing. Notably, our culture system also generated cDC2-like cells, based on the expression of CD1c and SIRPα. As our current study exclusively focused on characterizing the functionality of bulk progenitor-derived DC, it would be valuable to assess the individual potency of progenitor-derived cDC1- and cDC2-like cells, as well as their combination to orchestrate anti-tumor CTL responses. To achieve that, additional studies using mRNA sequencing may be needed to identify key cell surface markers to separate cDC1-like and cDC2-like cells generated *in vitro*. This is because the key markers used for identifying *ex vivo* DC subsets are less reliable for *in vitro* cultured cells[45].

The recent breakthroughs in the understanding of anti-tumor immune responses have opened a new era in cancer treatment. In addition to immune checkpoint blockade, T cell-based cancer immunotherapy has reached the clinic, using T cells endowed with chimeric antigen receptors (CAR) directed at cell surface antigens. In addition, use of T cells endowed with tumor antigen-specific TCRs is a heavily explored approach. For this form of adoptive cell therapy (ACT), the identification of tumor antigen-specific T cells is essential. These T cells can be used as such, or their TCRs can be isolated and transferred to recipient T cells that are sued for therapy. Tumor infiltrating lymphocytes (TIL) are a source of tumor-but peripheral blood is explored as alternative source[54,55].

Yossef *et al*.[38] have recently found that neoantigen-specific CD8$^+$ T-cells in the circulation share markers with TIL, while lacking features of terminal dysfunction. Therefore, circulating tumor-reactive CD8$^+$ T-cells may be leveraged for ACT, but their frequencies are generally very low[38–40]. At present, generally moDC are used to facilitate detection of tumor antigen-specific T-cells[38], in combination with staining with peptide/MHC multimers[56], and antibodies to effector cytokines[57] and/or T-cell activation markers[58,59]. However, the sensitivity of detection is still suboptimal[60]. Our "helped" cDC1 platform using trumor cell debris as antigen offers an opportunity for sensitive detection of tumor antigen-specific CD8+ T cells in blood of healthy donor or cancer patients that can be used for isolation of TCRs, or, in the case of cancer patients, for autologous ACT.

The TME is generally characterized by immune suppression, as mediated by specific cytokines, checkpoint receptors[61] and suppressive cells[62,63]. Furthermore, tumor-specific T-cells tend to become functionally "exhausted" in the TME due to chronic antigen stimulation[64,65]. Therefore, ACT will benefit from availability of optimally functional CTL[66]. CD4$^+$ T-cell help has been shown to improve CTL effector and memory differentiation in many aspects that are important for tumor elimination[23,24]. The presence of tumor-specific CD4$^+$ T-cells was found to correlate with response to MHC class II-negative tumors[67,68]. These findings are in accordance with DC-mediated CD4$^+$ T-cell help expanding and prolonging anti-tumor CTL responses[68]. We found that CD4$^+$ T-cell help delivered via progenitor-derived DC *in vitro* promoted CTL effector quality on a per cell basis. This approach may therefore be considered to make a more optimal T cell product for ACT.

To summarize, with the aid of our CTL priming platform, we demonstrate the ability of progenitor-derived DC to detect tumor antigen-specific T-cells in the blood of HLA-matched healthy donors even with low mutation burden, as indicated by both peptide/MHC tetramers and T-cell activation markers. Furthermore, we consistently observed an increase in the detection rate with the addition of DC-licensing via CD4$^+$ T-cell help. Thus, the cell culture system described here has the potential to broaden the scope of identifying tumor-reactive T-cells in the circulation for engineered TCR-based cell therapies, and to improve the fitness of current ACT. As this is a proof-of-concept study, several aspects remain to be addressed. It will be important to test additional samples from healthy individuals and cancer patients and to employ more specific peptide/MHC multimers[69] for further confirmation of the success rate of our approach in detecting tumor-reactive CD8$^+$ T-cells in the circulation. It will also be of interest to investigate whether the tumor-reactive T-cells (cross)primed by "helped/licensed" DC in our system can sustain their effector functions in the *in vivo* setting.

Materials and methods

Human peripheral blood samples

Human PBMC of healthy donors were obtained in accordance with the Declaration of Helsinki and the Dutch rules with respect to the use of human materials from volunteer donors. Buffy coats from anonymized healthy donors (HD) were obtained after their written informed consent, as approved by Sanquin's internal ethical board. PBMC were isolated from buffy coats using Ficoll-Paque Plus density gradient centrifugation (GE Healthcare) and cells were cryopreserved till further use. DC were isolated from HLA-A2$^+$ donors, while CD4$^+$ and CD8$^+$ T-cells used in this study were used regardless of their HLA type and were not necessarily from the same donor.

Cell lines

The Mel526 cell line originates from the S.A. Rosenberg laboratory (National Institutes of Health, Bethesda, USA, RRID:CVCL_8051). The OP9 stromal cell line expressing human DLL1 (OP9-hDLL1) was generated by retrovirally transducing OP9 stromal cell line with hDLL1. The construct was provided by the V. Bigley lab from Newcastle University.

Fluorescence-activated cell sorting (FACS)

CD19$^+$ cells were depleted from PBMC before sorting using CD19 magnetic MicroBeads (MACS), according to the manufacturer's protocol. Staining was performed at 4°C for 45 min in flow cytometry staining buffer (BD Biosciences). The following antibodies were used: from BioLegend: CD3 (clone OKT3), CD4 (clone OKT4), CD8 (clone SK1), CD19 (clone HIB19), CD25 (BC96), CD45RA (clone HI100), CD34 (clone 581), HLA-DR (clone L243); from BD Biosciences: HLA-DR (clone G46-6); from eBiosciences: CD117/c-Kit (clone 104D2). Near-IR Dead Cell Stain Kit (Invitrogen), Zombie Red Fixable Viability Kit (BioLegend) or 7-amino-actinomycin D (7-AAD, eBioscience) were used to exclude dead cells. In order to prevent clump formation from dead cells, 0.01% DNase (Invitrogen) was added before sorting. Cell sorting was performed on BD FACSAria III (BD Biosciences).

Flow cytometry

Cell surface staining: Staining was performed at 4°C for 30 min in flow cytometry staining buffer (BD Biosciences). The following antibodies were used: from BioLegend: CD1a (clone HL149), CD2 (clone RPA-2.10), CD3 (clone OKT3), CD19 (clone HIB19), CD11c (clone 3.9), CD14 (clone 63D3), CD40 (clone 5C3), CD70 (clone 113-16), CD80 (clone 2D10), CD83 (clone HB15e), CD86 (clone IT2.2), CD107α (clone H4A3), CD123 (clone 6H6, 1:30), CD141 (clone M80), CD163 (clone GHI/61), CD206 (clone 44972.00), CCR7 (clone G043H7), CLEC9A (clone 8F9, dilution 1:75), HLA-A2 (clone BB7.2), HLA-ABC (clone W6/32), HLA-DR (clone L243), XCR1 (clone S15046E), Sirpα (clone 15-414), DLL1 (clone MHD1-314); from BD Biosciences: CD1c (clone F10/21A3), CD3 (clone UCHT1), CD5 (clone L17F12), CD45RO (clone UCHL1), CD88 (clone D53-1473), CD163 (clone GHI/61), CD303 (clone V24-785), CLEC9A (clone 3A4), DLL1 (clone MHD1-314); from Miltenyi Biotec: CD141 (clone REA674). APC/AF488-conjugated HLA-A2/MART-1_{26-35} tetramers (dilution 1:30), APC/PE-conjugated HLA-A2/$CDK4_{23-32}$ tetramers (dilution 1:30), APC-conjugated HLA-A2/$gp100_{280-288}$ tetramer (dilution 1:30) and PE-conjugated HLA-A2/$MAGE3_{271-279}$ tetramer ((dilution 1:30) were added together with cell surface staining antibodies. Near-IR Dead Cell Stain Kit (dilution 1:1000, Invitrogen), Zombie Red Fixable Viability Kit (dilution 1:800, BioLegend), Zombie UV Fixable Viability Kit (dilution 1:800, BioLegend) or 7-Aminoactinomycin D (dilution 1:20, 7-AAD, eBiosciences) were used to discriminate between live and dead cells.

For intracellular staining, protein transport inhibitor (BD GolgiPlug) (1:1000) was added into the culture for 3 h before cells were harvested and analyzed by flow cytometry. After surface staining, cells were fixed and permeabilized using the BD Cytofix/Cytoperm kit (BD Biosciences), according to the manufacturer's protocol. Antibodies to the following molecules were used: from BioLegend: β2m (clone A17082A), CXCL9 (clone J1015E10), CXCL10 (clone J034D6), Granzyme B (clone QA16A02), IFNγ (clone B27); from Bioss: rabbit anti-human TAP1 and TAP2 polyclonal antibodies (dilution 1:100); from Thermo Fisher Scientific: IRF8 (clone V3GYWCH, dilution 1:75), goat anti-rabbit IgG(H+L) Alexa Fluor 488 (dilution 1:200) and goat anti-mouse IgG(H+L) Alexa Fluor 647 (dilution 1:300) secondary antibodies. Specific staining was confirmed by Fluorescence Minus One (FMO) control. Antibody stocks were diluted 1:50 for use unless stated otherwise. Flow cytometry was performed using a BD LSR Fortessa™ or Cytek Aurora spectral flow cytometer. Data were analysed using FlowJo™ software version 10.8.2 (BD Biosciences) or OMIQ software (Dotmatics).

In vitro generation of blood progenitor-derived DC

At 24 h before progenitor isolation, MSC and OP9-hDLL1 were harvested using 0.05% trypsin (Sigma). MSC and OP9-hDLL1 were irradiated at 16Gy and 30Gy respectively before seeding as feeder cells in Iscove's Modified Dulbecco's Medium (IMDM, Gibco) with 10% FBS, penicillin/streptomycin, β-mercaptoethanol in round-bottom 96-well plates (BD Falcon) at a density of 3000 cells/well. The ratio of MSC and OP9-hDLL1 was 3:1. Blood $Lin^{-}CD34^{+}c\text{-}Kit^{+}$ HPC were flow cytometrically sorted and seeded on the feeder cells at a density of 1000 cells/well in IMDM with 10% FBS at 5% CO_2 and 37°C. To expand and differentiate progenitors into DC, cells were incubated with additional cytokines at the final concentration of 100 ng/ml human (h)FLT3L (Miltenyi Biotec), 0.5 ng/ml hM-CSF (Miltenyi Biotec), 10 ng/ml hIL-7 (Miltenyi Biotec), 5 ng/ml hTPO (Miltenyi Biotec), 5 ng/ml hSCF (Miltenyi Biotec) and 1 ng/ml hGM-CSF (Miltenyi Biotec). Cells were cultured for 14 days before use in phenotyping or functional assays.

Tumor antigen-specific CTL priming platform

This method was adapted from a protocol described in our previous publication[19]. $CD8^{+}$ T-cells used in Figure 3 were retrovirally transduced with MART-$1_{26\text{-}35}$/HLA-A2-specific TCR according to a protocol described in our previous publication[19]. $CD8^{+}$ T-cells used in Figure 4 and 5 were purified total $CD8^{+}$ T-cells without TCR transduction. Briefly, sorted $HLA\text{-}DR^{-}CD3^{+}CD8^{+}$ T-cells were cultured in RPMI-1640, supplemented with 10% FBS, penicillin/streptomycin, β-mercaptoethanol, in the presence hIL-2, hIL-7 and hIL-15 (Miltenyi Biotec) each at 10 ng/ml for 10-14 days, then used in *in vitro* CTL priming experiments. For Figure 3, MART-$1_{26\text{-}35}$ short peptide (ELAGIGILTV, 500ng/ml), MART-$1_{15\text{-}40}$ long peptide (KGHGHSYTTAEELAGIGILTV, 20 mg/ml) or dead Mel526 cell debris was used; For Figure 4 and 5, dead Mel526 cell debris was used. Mel526 cells were treated with 100 ng/ml tumour necrosis factor-related apoptosis-inducing ligand (TRAIL, Sigma) and 10 ng/ml Fas Ligand (FASL, AdipoGen) to induce apoptotic cell death. $HLA\text{-}A2^{+}$ progenitor-derived DC were incubated with activated- or naïve $CD4^{+}$ T-cells in 1 DC: 1 $CD4^{+}$ T-cell ratio for 2 h in IMDM, supplemented with 1% FBS, after which tumor antigens were added. After 12-16 h, cell supernatant was washed away. Next, $CD8^{+}$ T-cells were added into the culture in a ratio of 1 DC per 10 $CD8^{+}$ T-cells and cultured for 6-7 days in RPMI-1640, supplemented with 10% FBS and 0.2 ng/ml hIL-7/hIL-15. To trace proliferation, $CD8^{+}$ T-cells were labeled with CTV before being added into the CTL priming assay. 50 ng/ml Phorbol 12-myristate 13-acetate

(PMA, Sigma), 1 mg/ml Ionomycin (InvivoGen) and Protein transport inhibitor (BD GolgiPlug, 1:1000) were added into the culture for 3 h before cells were harvested and analyzed by flow cytometry.

IncuCyte T-cell killing assay

One day before the killing assay, live melanoma (Mel526) cells were plated in a 96-well flat bottom black wall plates (Greiner) at a density of 5,000 cells/well. Mel526 cells were passed through G21 needles (BD Biosciences) before plating to avoid aggregation. The following day, growth medium was removed and 100 µl IncuCyte® Caspase-3/7 Green Apoptosis Reagent (20 µM, Sartorius) was added. Then $CD8^+$ T-cells isolated from the tumor antigen-specific CTL priming platform using flow cytometric sorting were seeded in 100 µl medium into the appropriate wells at effector : target (E:T) ratio of 4:1. The assay plate was settled on a level surface at ambient temperature for 30 min before being placed into the IncuCyte live-cell analysis system (IncuCyte ZOOM®, Sartorius). Plates were scanned every 2 h for 24 h. Afterwards, the cell suspension was collected and analyzed by flow cytometry, and remaining Mel526 cells were fixed by 4% PFA (Sigma), stained with crystal violet and imaged by charge-coupled device (CCD) microscope Zeiss Axio Imager Z1. IncuCyte data was analyzed with IncuCyte® S3 Software (version 2018B).

Statistical analysis

Data, excluding those describing mRNA sequencing using public datasets and IncuCyte killing assay, were analyzed using GraphPad Prism (version 9.0). Student’s t test or one-Way ANOVA was used to determine significant differences between samples or groups. Data are represented as means ±SEM. P value < 0.05 was considered statistically significant.

Materials and data availability

This study did not generate new unique reagents. Software used to analyze sequencing data is publicly available. Other primary data and materials that support the findings of this study are available from the corresponding author upon reasonable request.

Acknowledgements

This collaboration project was funded by an Antoni van Leeuwenhoek Foundation grant from the Bakker family to J.B. and Y.X. It was additionally funded by the PPP Allowance to J.B., Y. X. and H.v.E. made available by Health~Holland, Top Sector Life Sciences & Health, to stimulate public-private partnerships; Oncode to J.B.; Dutch Cancer Society (KWF) grant 11079 to J.B. and Y.X.. We thank all personnel of the flow cytometry facilities at the Netherlands Cancer Institute and Leiden University Medical Center for their excellent technique support. We thank C.L.M.C. Franken, E. de Vries and Lenny Brocks for assistance. Images for clipart used figures are derived from BioRender.com.

Author contributions

X.L. designed and performed experiments, analyzed data and wrote the manuscript. Y.W. contributed to performing experiments, analyzing data and writing manuscript. T.d.W. contributed to cell sorting and co-culture experiments. J. van den B. and M.B. contributed to sample collection and performed experiments. J.W. contributed to peptide synthesis and provided insight. C.S. contributed to experiments and provided insight. N.F.C.M. provided insight. T.S. provided the construct encoding the MART-1-specific TCR and provided insight. J.B interpreted data, provided insight and wrote the manuscript; Y.X. designed the research, performed experiment, analyzed/interpreted data and wrote the manuscript.

Competing Interests Statement

The authors declare that the research was conducted in the absence of any commercial or financial relationships that could be construed as a potential conflict of interest.

References

1. Reis e Sousa, C. Dendritic cells in a mature age. *Nat Rev Immunol* **6**, 476–483 (2006).
2. Pulendran, B. The Varieties of Immunological Experience: Of Pathogens, Stress, and Dendritic Cells. *Annu Rev Immunol* **33**, 563–606 (2015).
3. Merad, M., Sathe, P., Helft, J., Miller, J. & Mortha, A. The Dendritic Cell Lineage: Ontogeny and Function of Dendritic Cells and Their Subsets in the Steady State and the Inflamed Setting. *Annu Rev Immunol* **31**, 563–604 (2013).
4. Segura, E. Human dendritic cell subsets: An updated view of their ontogeny and functional specialization. *Eur J Immunol* **52**, 1759–1767 (2022).
5. Collin, M. & Bigley, V. Human dendritic cell subsets: an update. *Immunology* **154**, 3–20 (2018).
6. Karsunky, H., Merad, M., Cozzio, A., Weissman, I. L. & Manz, M. G. Flt3 Ligand Regulates Dendritic Cell Development from Flt3+ Lymphoid and Myeloid-committed Progenitors to Flt3+ Dendritic Cells In Vivo. *J Exp Med* **198**, 305–313 (2003).
7. Dutertre, C.-A. *et al.* Single-Cell Analysis of Human Mononuclear Phagocytes Reveals Subset-Defining Markers and Identifies Circulating Inflammatory Dendritic Cells. *Immunity* **51**, 573-589.e8 (2019).
8. Villani, A.-C. *et al.* Single-cell RNA-seq reveals new types of human blood dendritic cells, monocytes, and progenitors. *Science (1979)* **356**, eaah4573 (2017).
9. Murphy, K. M. Transcriptional Control of Dendritic Cell Development. *Annu Rev Immunol* **34**, 93–119 (2016).
10. Cytlak, U. *et al.* Differential IRF8 Transcription Factor Requirement Defines Two Pathways of Dendritic Cell Development in Humans. *Immunity* **53**, 353-370 (2020).
11. Durand, M. & Segura, E. The Known Unknowns of the Human Dendritic Cell Network. *Front Immunol* **6**, (2015).
12. Broz, M. L. & Krummel, M. F. The Emerging Understanding of Myeloid Cells as Partners and Targets in Tumor Rejection. *Cancer Immunol Res* **3**, 313–319 (2015).
13. Roberts, E. W. *et al.* Critical Role for CD103 + /CD141 + Dendritic Cells Bearing CCR7 for Tumor Antigen Trafficking and Priming of T Cell Immunity in Melanoma. *Cancer Cell* **30**, 324–336 (2016).
14. den Haan, J. M. M., Lehar, S. M. & Bevan, M. J. Cd8+ but Not Cd8− Dendritic Cells Cross-Prime Cytotoxic T Cells in Vivo. *Journal of Experimental Medicine* **192**, 1685-96 (2000).
15. Schenkel, J. M. *et al.* Conventional type I dendritic cells maintain a reservoir of proliferative tumor-antigen specific TCF-1+ CD8+ T cells in tumor-draining lymph nodes. *Immunity* **54**, 2338-2353.e6 (2021).
16. Burger, M. L. *et al.* Antigen dominance hierarchies shape TCF1+ progenitor CD8 T cell phenotypes in tumors. *Cell* **184**, 4996-5014.e26 (2021).
17. Duraiswamy, J. *et al.* Myeloid antigen-presenting cell niches sustain antitumor T cells and license PD-1 blockade via CD28 costimulation. *Cancer Cell* **39**, 1623-1642.e20 (2021).
18. Prokhnevska, N. *et al.* CD8+ T cell activation in cancer comprises an initial activation phase in lymph nodes followed by effector differentiation within the tumor. *Immunity* **56**, 107-124. e5 (2023).

19. Lei, X. *et al.* CD4+ helper T cells endow cDC1 with cancer-impeding functions in the human tumor micro-environment. *Nat Commun* **14**, (2023).
20. Wu, R. *et al.* Mechanisms of CD40-dependent cDC1 licensing beyond costimulation. *Nat Immunol* **23**, 1536–1550 (2022).
21. Borst, J., Ahrends, T., Bąbała, N., Melief, C. J. M. & Kastenmüller, W. CD4+ T cell help in cancer immunology and immunotherapy. *Nat Rev Immunol* **18**, (2018).
22. Ferris, S. T. *et al.* cDC1 prime and are licensed by CD4+ T cells to induce anti-tumour immunity. *Nature* **584**, 624–629 (2020).
23. Ahrends, T. *et al.* CD4+ T Cell Help Confers a Cytotoxic T Cell Effector Program Including Coinhibitory Receptor Downregulation and Increased Tissue Invasiveness. *Immunity* **47**, 848-861.e5 (2017).
24. Ahrends, T. *et al.* CD4+ T cell help creates memory CD8+ T cells with innate and help-independent recall capacities. *Nat Commun* **10**, 5531 (2019).
25. Spranger, S., Dai, D., Horton, B. & Gajewski, T. F. Tumor-Residing Batf3 Dendritic Cells Are Required for Effector T Cell Trafficking and Adoptive T Cell Therapy. *Cancer Cell* **31**, 711-723.e4 (2017).
26. Meiser, P. *et al.* A distinct stimulatory cDC1 subpopulation amplifies CD8+ T cell responses in tumors for protective anti-cancer immunity. *Cancer Cell* **41**, 1498-1515.e10 (2023).
27. Oh, S. A. *et al.* PD-L1 expression by dendritic cells is a key regulator of T-cell immunity in cancer. *Nat Cancer* **1**, 681–691 (2020).
28. Larkin, J. *et al.* Five-Year Survival with Combined Nivolumab and Ipilimumab in Advanced Melanoma. *New England Journal of Medicine* **381**, 1535–1546 (2019).
29. Garon, E. B. *et al.* Pembrolizumab for the Treatment of Non–Small-Cell Lung Cancer. *New England Journal of Medicine* **372**, 2018–2028 (2015).
30. Hamid, O. *et al.* Five-year survival outcomes for patients with advanced melanoma treated with pembrolizumab in KEYNOTE-001. *Annals of Oncology* **30**, 582–588 (2019).
31. Luca, B. A. *et al.* Atlas of clinically distinct cell states and ecosystems across human solid tumors. *Cell* **184**, 5482-5496.e28 (2021).
32. Rosenberg, S. A. & Restifo, N. P. Adoptive cell transfer as personalized immunotherapy for human cancer. *Science (1979)* **348**, 62–68 (2015).
33. Zhao, Q. *et al.* Engineered TCR-T Cell Immunotherapy in Anticancer Precision Medicine: Pros and Cons. *Front Immunol* **12**, (2021).
34. Cohen, C. J. *et al.* Isolation of neoantigen-specific T cells from tumor and peripheral lymphocytes. *Journal of Clinical Investigation* **125**, 3981–3991 (2015).
35. Simoni, Y. *et al.* Bystander CD8+ T cells are abundant and phenotypically distinct in human tumour infiltrates. *Nature* **557**, 575–579 (2018).
36. Gros, A. *et al.* Recognition of human gastrointestinal cancer neoantigens by circulating PD-1+ lymphocytes. *Journal of Clinical Investigation* **129**, 4992–5004 (2019).
37. van den Bulk, J. *et al.* Neoantigen-specific immunity in low mutation burden colorectal cancers of the consensus molecular subtype 4. *Genome Med* **11**, 87 (2019).
38. Yossef, R. *et al.* Phenotypic signatures of circulating neoantigen-reactive CD8+ T cells in patients with metastatic cancers. *Cancer Cell* **41**, 2154-2165.e5 (2023).

39. Malekzadeh, P. *et al.* Antigen Experienced T Cells from Peripheral Blood Recognize p53 Neoantigens. *Clinical Cancer Research* **26**, 1267–1276 (2020).
40. Cafri, G. *et al.* Memory T cells targeting oncogenic mutations detected in peripheral blood of epithelial cancer patients. *Nat Commun* **10**, 449 (2019).
41. Blank, C. U., Haanen, J. B., Ribas, A. & Schumacher, T. N. The “cancer immunogram”. *Science (1979)* **352**, 658–660 (2016).
42. Fesnak, A. D., June, C. H. & Levine, B. L. Engineered T cells: the promise and challenges of cancer immunotherapy. *Nat Rev Cancer* **16**, 566–581 (2016).
43. O’Donnell, J. S., Teng, M. W. L. & Smyth, M. J. Cancer immunoediting and resistance to T cell-based immunotherapy. *Nat Rev Clin Oncol* **16**, 151–167 (2019).
44. Kirkling, M. E. *et al.* Notch Signaling Facilitates In Vitro Generation of Cross-Presenting Classical Dendritic Cells. *Cell Rep* **23**, 3658-3672.e6 (2018).
45. Balan, S. *et al.* Large-Scale Human Dendritic Cell Differentiation Revealing Notch-Dependent Lineage Bifurcation and Heterogeneity. *Cell Rep* **24**, 1902-1915.e6 (2018).
46. Horwitz, Edwin M., Andreef, M. & Frassoni, F. Mesenchymal stromal cells. *Curr Opin Hematol* **13**, 419–425 (2006).
47. Majumdar, M. K., Thiede, M. A., Mosca, J. D., Moorman, M. & Gerson, S. L. Phenotypic and functional comparison of cultures of marrow-derived mesenchymal stem cells (MSCs) and stromal cells. *J Cell Physiol* **176**, 57–66 (1998).
48. Xiao, Y. *et al.* Identification of the Common Origins of Osteoclasts, Macrophages, and Dendritic Cells in Human Hematopoiesis. *Stem Cell Reports* **4**, 984–994 (2015).
49. van Eck van der Sluijs, J. *et al.* Clinically applicable CD34+-derived blood dendritic cell subsets exhibit key subset-specific features and potently boost anti-tumor T and NK cell responses. *Cancer Immunology, Immunotherapy* **70**, 3167–3181 (2021).
50. Wu, R. *et al.* Mechanisms of CD40-dependent cDC1 licensing beyond costimulation. *Nat Immunol* **23**, 1536–1550 (2022).
51. Adema, G. J., de Vries, I. J. M., Punt, C. J. & Figdor, C. G. Migration of dendritic cell based cancer vaccines: in vivo veritas? *Curr Opin Immunol* **17**, 170–174 (2005).
52. Plantinga, M. *et al.* Conventional and Monocyte-Derived CD11b+ Dendritic Cells Initiate and Maintain T Helper 2 Cell-Mediated Immunity to House Dust Mite Allergen. *Immunity* **38**, 322–335 (2013).
53. Noubade, R., Majri-Morrison, S. & Tarbell, K. V. Beyond cDC1: Emerging Roles of DC Crosstalk in Cancer Immunity. *Front Immunol* **10**, (2019).
54. Verdegaal, E. M. E. *et al.* Successful treatment of metastatic melanoma by adoptive transfer of blood-derived polyclonal tumor-specific CD4+ and CD8+ T cells in combination with low-dose interferon-alpha. *Cancer Immunology, Immunotherapy* **60**, 953–963 (2011).
55. Verdegaal, E. M. E. *et al.* Timed adoptive T cell transfer during chemotherapy in patients with recurrent platinum-sensitive epithelial ovarian cancer. *J Immunother Cancer* **11**, e007697 (2023).
56. Arnaud, M. *et al.* Biotechnologies to tackle the challenge of neoantigen identification. *Curr Opin Biotechnol* **65**, 52–59 (2020).

57. Dijkstra, K. K. *et al.* Generation of Tumor-Reactive T Cells by Co-culture of Peripheral Blood Lymphocytes and Tumor Organoids. *Cell* **174**, 1586-1598.e12 (2018).

58. Seliktar-Ofir, S. *et al.* Selection of Shared and Neoantigen-Reactive T Cells for Adoptive Cell Therapy Based on CD137 Separation. *Front Immunol* **8**, (2017).

59. Tran, E., Robbins, P. F. & Rosenberg, S. A. 'Final common pathway' of human cancer immunotherapy: targeting random somatic mutations. *Nat Immunol* **18**, 255–262 (2017).

60. Lang, F., Schrörs, B., Löwer, M., Türeci, Ö. & Sahin, U. Identification of neoantigens for individualized therapeutic cancer vaccines. *Nat Rev Drug Discov* **21**, 261–282 (2022).

61. Sharma, P., Hu-Lieskovan, S., Wargo, J. A. & Ribas, A. Primary, Adaptive, and Acquired Resistance to Cancer Immunotherapy. *Cell* **168**, 707–723 (2017).

62. Ruffell, B. & Coussens, L. M. Macrophages and Therapeutic Resistance in Cancer. *Cancer Cell* **27**, 462–472 (2015).

63. Tanaka, A. & Sakaguchi, S. Targeting Treg cells in cancer immunotherapy. *Eur J Immunol* **49**, 1140–1146 (2019).

64. van der Leun, A. M., Thommen, D. S. & Schumacher, T. N. CD8+ T cell states in human cancer: insights from single-cell analysis. *Nat Rev Cancer* **20**, 218–232 (2020).

65. Philip, M. & Schietinger, A. CD8+ T cell differentiation and dysfunction in cancer. *Nat Rev Immunol* **22**, 209–223 (2022).

66. Jafarzadeh, L., Masoumi, E., Fallah-Mehrjardi, K., Mirzaei, H. R. & Hadjati, J. Prolonged Persistence of Chimeric Antigen Receptor (CAR) T Cell in Adoptive Cancer Immunotherapy: Challenges and Ways Forward. *Front Immunol* **11**, (2020).

67. Kreiter, S. *et al.* Mutant MHC class II epitopes drive therapeutic immune responses to cancer. *Nature* **520**, 692–696 (2015).

68. Alspach, E. *et al.* MHC-II neoantigens shape tumour immunity and response to immunotherapy. *Nature* **574**, 696–701 (2019).

69. Mallajosyula, V. *et al.* CD8 $^{+}$ T cells specific for conserved coronavirus epitopes correlate with milder disease in patients with COVID-19. *Sci Immunol* **6**, (2021).

Supplementary Information

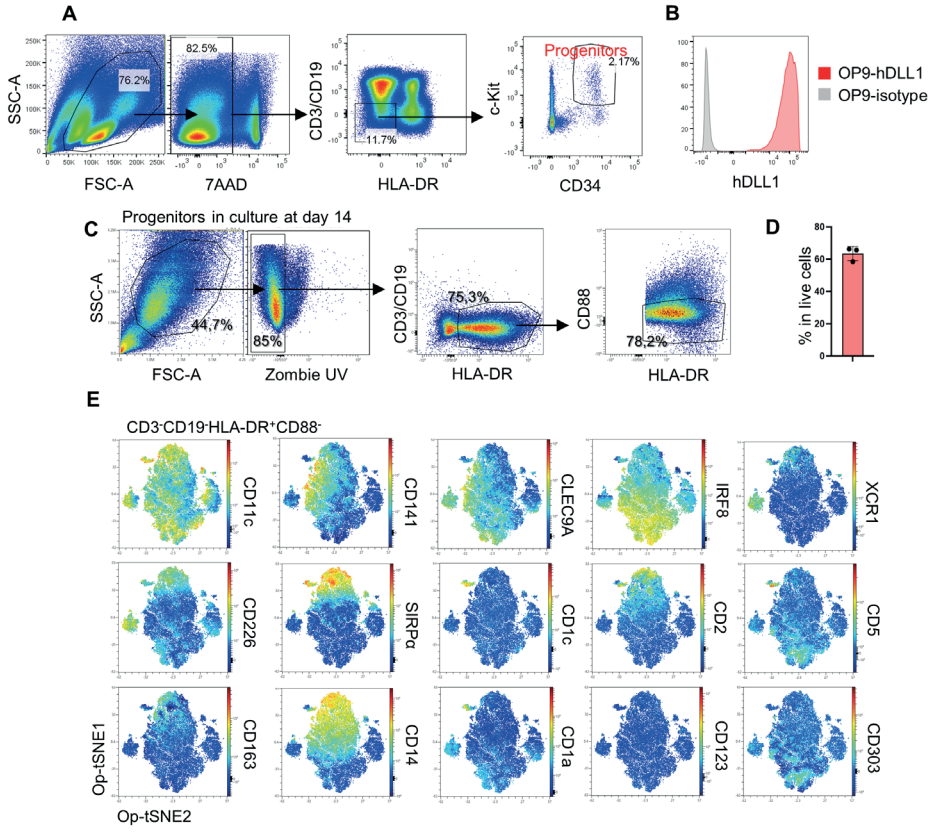

Fig. S1 Generating human cDC1-like cells from non-mobilized blood-derived progenitors in vitro. (**A**) Gating strategy for progenitor cells isolation from PBMC. (**B**) Histogram depict the expression of hDLL1 by OP9 stromal cell line. (**C**) Gating strategy for progenitor-derived DC phenotype analysis. (**D**) Quantification of frequencies (%) of $CD3^{-}CD19^{-}HLA\text{-}DR^{+}CD88^{-}$ DC progeny in live cells. (**E**) Op-tSNE plots depict expression of indicated markers on $CD3^{-}CD19^{-}HLA\text{-}DR^{+}CD88^{-}$ population.

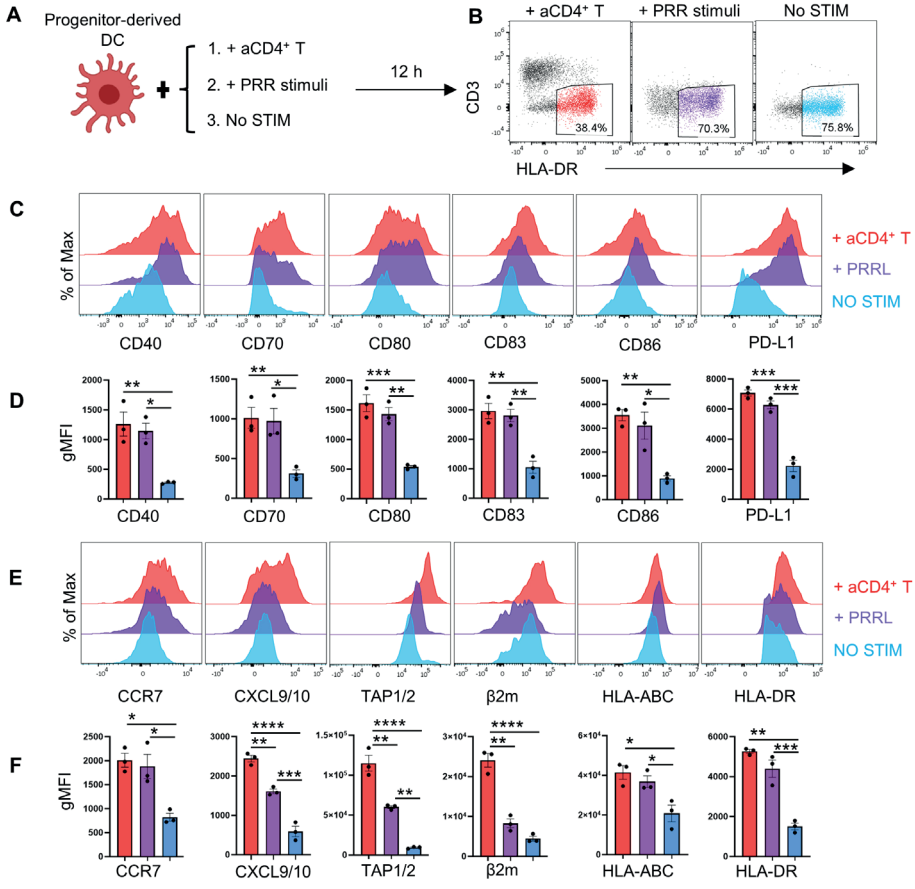

Fig. S2 Progenitor-derived DC are activated upon CD4+ T-cell and pattern recognition receptor ligand stimulation. Progenitor-derived DC were co-cultured with activated (a)CD4+ T-cells or a mixture of TLR3, -4, and -7/8 agonists overnight, as specified in our previous study[19]. Next, key molecules of the cDC1 "help" signature were analyzed by flow cytometry[19]. (**A**) Illustration of the experimental design. (**B**) Gating strategy for flow cytometric analysis of progenitor-derived DC after co-culture. (**C-F**) Histograms (**C** and **E**) and geometric mean fluorescent index (gMFI) quantifications (**D** and **F**) for indicated markers expressed by progenitor-derived DC under indicated conditions. Data are pooled from three (n=3) independent donors in **D** and **F**, and are shown as means ± SEM. p<0.05*, p<0.01**, p<0.001*** (two-sided unpaired student t test).

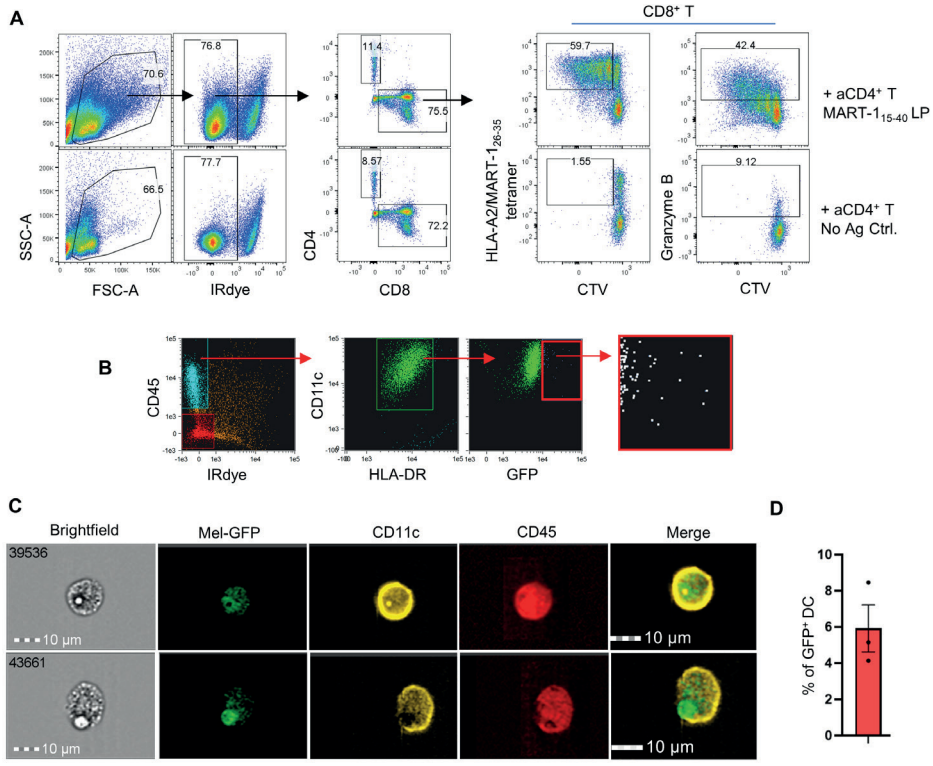

Fig. S3 Progenitor-derived DC has the ability to relay CD4⁺ T-cell help for CTL responses. (**A**) Gating strategies for detecting CD8⁺ T-cell responses in our in vitro cytotoxic T-cell priming system based on CTV dilution and intracellular Granzyme B staining. CD8⁺ T-cells had been transduced to express the HLA-A2/MART-1_{26-35}-specific TCR before being added to priming system. (**B-D**) Imaging flow cytometry was performed to analyze the phagocytotic capacity of progenitor-derived DC. (**B**) Gating strategy for analyzing phagocytotic capacity of progenitor-derived DC response. (**C**) Representative brightfield and fluorescent images of CD11c⁺CD45⁺ progenitor-derived DC phagocytosing GFP⁺ melanoma cell debris. (**D**) Quantification of % of GFP⁺ cells in total live DC. Data are pooled from three (n=3) independent donors in **D**, and are shown as means ± SEM.

A

Peptide ID	*Peptide sequence*	*HLA allele*	*Fluorochrome*
MART-1_{25-36}	ELAGYGILTV	HLA-A0201	AF488 & APC
$CDK4_{23-32}$	ALDPHSGHFV	HLA-A0201	APC & PE
$gp100_{280-288}$	YLEPGPVTA	HLA-A0201	APC
MAGE3	FLWGPRALV	HLA-A0201	PE

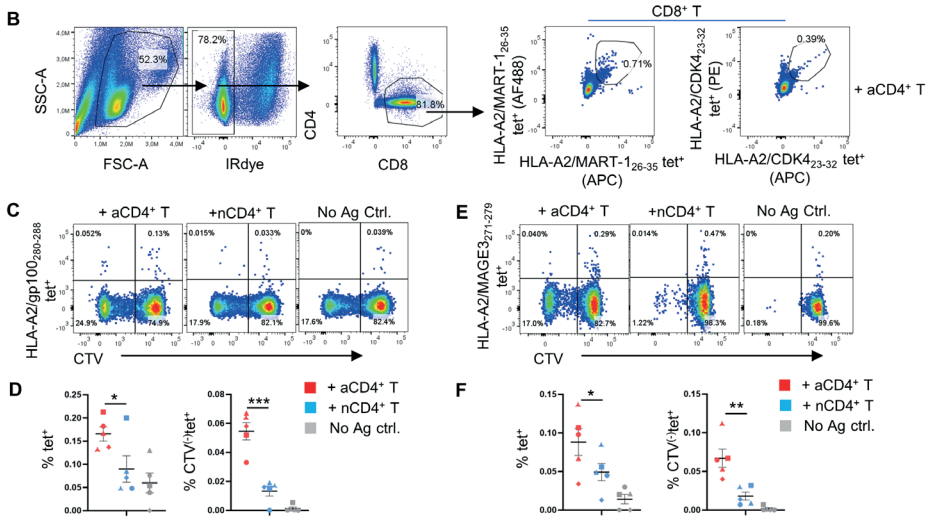

Fig. S4 Progenitor-derived DC can detect tumor antigen-specific CD8⁺ T-cells in blood. CTV labeled CD8⁺ T-cells were co-cultured with progenitor-derived DC loaded with dead Mel526 cell debris in presence of activated (a)- or naïve (n)CD4⁺ T-cells. Tumor antigen-specific CD8⁺ T-cells were detected using peptide/MHC-I tetramers. (**A**) Overview of the tetramers used in the experiment(s). (**B**) Gating strategy for detecting tumor antigen-specific CD8⁺ T-cells using tetramers. (**C** and **E**) Flow cytometric plots depict CD8⁺ T-cells specific for (**C**) HLA-A2/$gp100_{280-288}$ and (**E**) HLA-A2/$MAGE3_{271-279}$. (**D** and **F**) Quantification % (**D**) $gp100_{280-288}$-specific and (**F**) $MAGE3_{271-279}$-specific population within CD8⁺ T-cells (left), and # of (**D**) $gp100_{280-288}$-specific and (**F**) $MAGE3_{271-279}$-specific CD8⁺ T-cells (right). Data are pooled from five (n=5) healthy donors and are shown as means ± SEM. $p<0.05$*, $p<0.01$**, $p<0.001$*** (two-sided unpaired student t test).

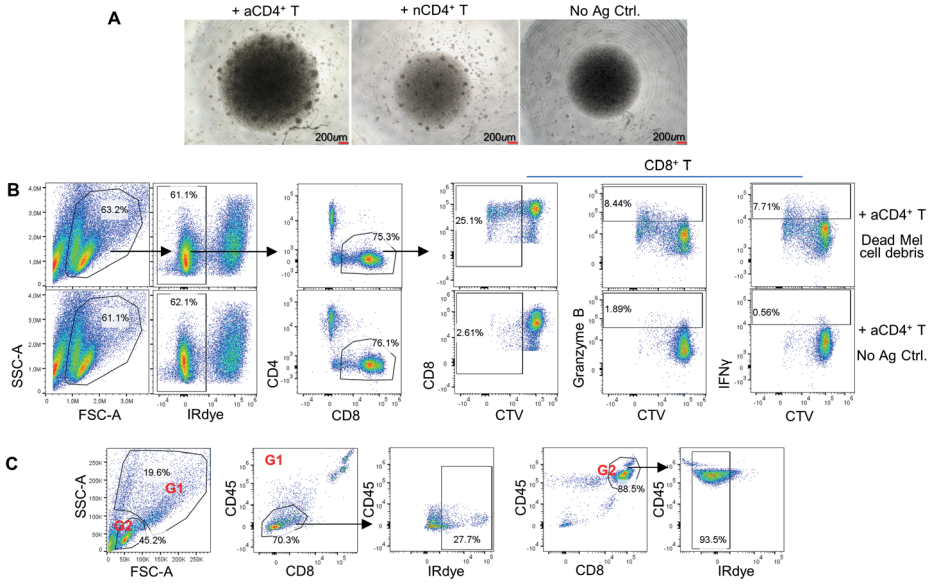

Fig. S5 “Licensed/helped” progenitor-derived DC prime CTL that exhibit enhanced anti-tumor function. CD8$^+$ T-cells were sorted from PBMC and co-cultured with progenitor-derived DC loaded with dead Mel526 cell debris in presence of activated (a)- or naïve (n)CD4$^+$ T-cells. Then CD8$^+$ T-cell response was measured at day 6 after co-culture by flow cytometry or subjected to killing assay. (A) Representative microscopic images depict CD8$^+$ T-cells 6 days after co-culture. (**B**) Gating strategies for detecting CD8$^+$ T-cell responses in our in vitro cytotoxic T-cell priming system based on CTV dilution, and intracellular Granzyme B and IFNγ staining. (**C**) Gating strategies for cells in suspension collected at the end of killing assay.

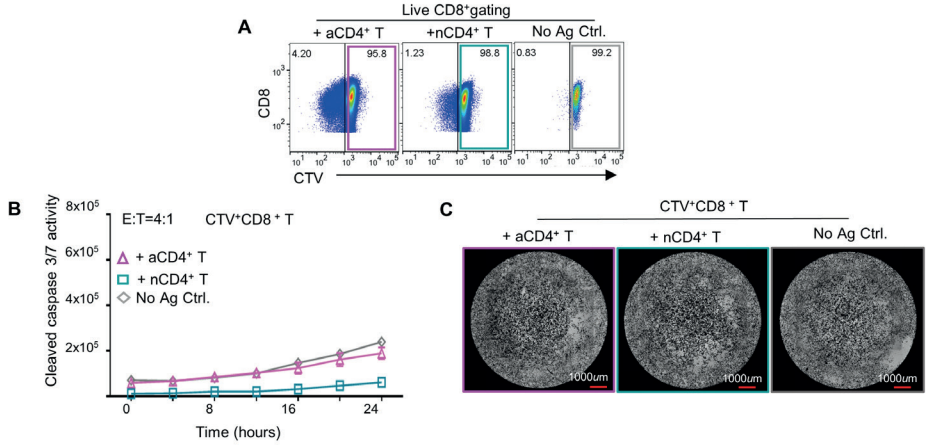

Fig. S6 Non-proliferative CTV⁺CD8⁺ T-cells have limited tumor cell killing capacity. CD8⁺ T-cells were sorted from PBMC and co-cultured with progenitor-derived DC loaded with dead Mel526 cell debris in presence of activated (a)- or naïve (n)CD4⁺ T-cells. Then, killing assay was performed using non-proliferative (CTV⁺) CD8⁺ T-cells purified from the priming system and Mel526 tumor cells at effector/target (E/T) ratio of 4/1, and analyzed by IncuCyte during 24h. At the end of the assay, remaining Mel526 cells in each well from all conditions were fixed and stained with crystal violet. (**A**) Gating strategy for isolating CTV⁺CD8⁺ T-cells from the CTL priming system. CTV⁺CD8⁺ T-cells without encountering antigen were used as control. Purple, teal and grey boxes highlight isolated T-cell population. (**B**) Cleaved caspase 3/7 activity in tumor cells during killing assay under indicated conditions. (**E**) Representative CCD microscopic images depicting remaining Mel526 cells in the plate at 24h post co-culture under indicated conditions. Data are pooled from two (n=2) independent donors, are shown as means ± SD.